PBG-SLAB EMBEDDED TRAVELING WAVE STRUCTURE FOR PLANAR BEAM ACCELERATOR APPLICATION *

Young-Min Shin, Department of Physics, Northern Illinois University, Dekalb, IL, 60115, USA and Accelerator Physics Center (APC), FNAL, Batavia, IL 60510, USA

Abstract

The oversized traveling wave (TE_{10}-mode) channel integrated with the photonic-band-gap (PBG) slab arrays have been investigated for planar beam accelerator application. Simulation analysis showed that the slab arrays allow only the PBG-modes (5 ~ 6 GHz) to propagate with ~ 2 dB of insertion loss, corresponding to ~ 1.14 dB/cm attenuation, which thereby effectively suppresses trapped non-PBG modes down to ~ - 14.3 dB/cm. It will enable monochromatic propagation of fundamental acceleration modes along the heavily over-moded planar waveguide without anomalous excitation of unstable trapped HOMs. The saturated maximum field gradients of the accelerating structure have been analyzed with respect to operational frequency bands corresponding to structural sizes. The field gradient of the guided PBG-mode has been investigated with finite-integral-method (FIM) simulations at W-band. The quasi-optical mode-selective traveling wave structure can efficiently mitigate a beam-breakup problem as lowering the beam-loading with increase of transverse geometrical aspect ratio. This mode-filter could be utilized for HOM dampers in high aspect ratio (HAR) planar beam accelerators. An experimental test is currently under consideration.

INTRODUCTION

Guided traveling waves bunch low energy particles, when their charge density exceeds thermo-dynamic divergence ($\propto f^2$) [1], which are commonly used for high intensity photon generation or high gradient RF acceleration. The operational spectral range of the coherent RF structures has rapidly increased from microwave to near-terahertz (near-THz) wave regime (0.1 ~ 1 THz) as device size is significantly reduced proportional to wavelength and repetition rate of the optical cycle on the photon-emission or -absorption is noticeably increased [2], [3]. Recent trends on development of THz electron beam devices have gradually transitioned to an elliptical planar beam from a round one as enlarging the beam width either increases radiation intensity or reduces beam-loading, mitigating beam-breakup instability. Among various planar slow wave structures [4 – 7], the micro-channel with asymmetrically aligned double grating array [8], [9] was intensively studied for frequency-tunable coherent radiation source application as exciting multi-chromatic plasmonic modes that are strongly confined in the beam channel with small ohmic losses over the fundamental pass-band. However, this broad band characteristic can lead to abnormal excitation and amplification of trapped HOMs, which possibly destabilize beam-wave interaction, perturbing normal electronic energy conversion. In particular, the structure becomes heavily over-moded (TE → TEM) as its structural aspect ratio between the transverse dimensions is increased to expand beam-wave interactive area. It is thus certain that there is a limit to increasing the geometrical aspect ratio of the transverse dimensions due to non-acceleration mode excitation in the heavily over-moded waveguide. A substantial solution to the issue could be obtained from band-pass filters. This paper will present the oversized slow wave channel integrated with the PBG-slab array. The hybrid structure permits only PBG-modes [10], [11] to propagate through the beam channel between the staggered sub-wavelength PBG slab arrays. Comparative numerical analysis on the spectral response and field distribution will be discussed in detail.

PC-SLAB WAVEGUIDE

The lowest frequency (cutoff) of a rectangular TE-mode waveguide is determined by waveguide width, so TE modes become closer to TEM ones as the cutoff is lowered. Figure 1 shows the 1st order dispersion curves of TE- and TEM-waveguides. Normalized structural dimensions of the designed models are specified with a/d = 0.75, L/d = 0.587, b/d = 0.326, and h/d = 1.674 and the surface wall conductivity is defined with OFHC (Oxygen-Free High-Conductivity) copper ($\sigma = 5.8 \times 10^8$ [$\Omega^{-1}m^{-1}$]). The passband of the 2nd TEM SWS (higher aspect ratio) thus tend to become more heavily overmoded with larger phase and group velocities.

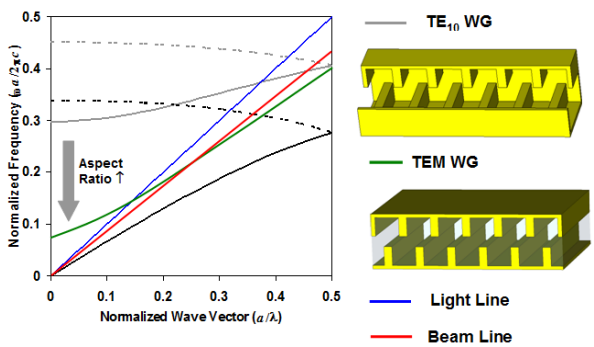

Figure 1: Dispersion curves of the staggered grating array structures (TE_{10}- and TEM-modes).

ISBN 978-3-95450-115-1

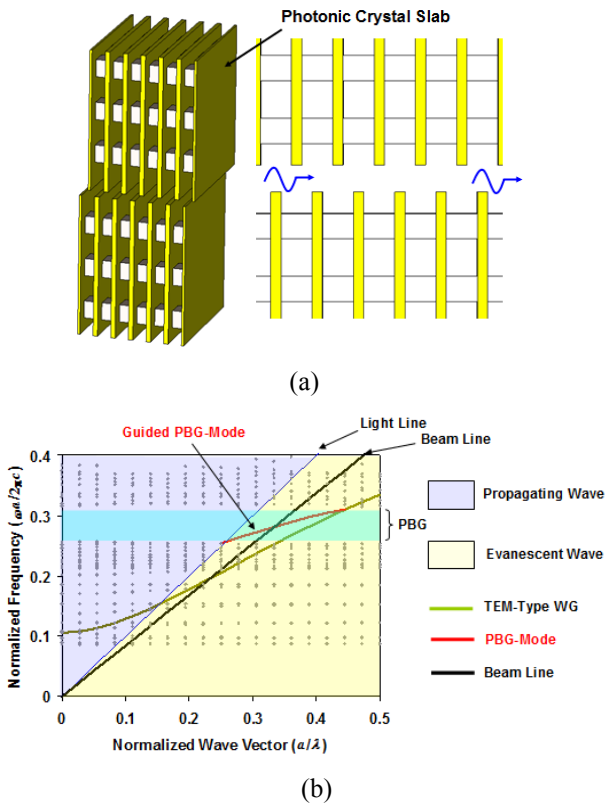

Figure 2: (a) staggered PC-slab array travelling wave accelerating structure (b) normalized dispersion graph.

Spatial harmonic components of lower frequency modes are readily coupled with low energy kinetic electrons, so that while haunting around in the structure, once excited, they are often self-amplified by phase-mismatching condition, which can cause strong perturbation to system operation.

Embodiment of PBG elements in guided wave structures is effective in suppressing low-energy trapped modes and HOMs in an active spectral band. In Fig. 2(a), the top and bottom gratings are replaced with the photonic-band-gap (PBG) slab arrays, which consist of lossy aluminum (Al_2O_3) rods. In the crystal slab designed with the lattice constant of $a/\lambda \sim 0.3$ and filling ratio of $r/a \sim 0.25$, a normalized global band-gap emerges at f (norm) = 0.25 ~ 0.3. Like an ordinary confined slow wave structure, EM waves bouncing back from the crystal lattices in the band-gap spectra that satisfy the Bragg condition propagate through the channel between the two PBG slab-arrays with strong field confinement. On the other hand, non-resonant eigenmodes outside the band gaps are freely radiated through the lattices, which are thereby strongly suppressed in the channel. It is evident that only the non-radiative plasmon modes in the band gap synchronously couple with electrons if the kinetic energy satisfies the coupling condition, $\gamma = \omega / ck_{sp}\big|_{m=1}$, of the PBG modes (gray-shaded area), where γ is the relativistic factor, $\gamma = \sqrt{1-(1+\sigma)^{-2}}$, and $\sigma = V_e/V_n$ ($V_n = m_e c^2/e = 5.11 \times 10^5$ [V]). The PBG-slab waveguide in Fig. 2(a) is designed to be so wide as to be highly over-moded, which leads to lowering cutoff frequency ($\omega a/2\pi c$ = 0.105). In this model, both lateral sides of the PBG-slabs are completely covered by the metal plates, so that eigenmodes only exist above the cutoff of fundamental-passband. Figure 2(b) compares the dispersion curves of the two slow waveguide structures with the staggered grating arrays and the PBG slabs that are procured by the finite-integral-method (FIM) eigenmode solver [12]. The blue-shaded and yellow-shaded areas represent the photonic zone (far-field, $k < 2\pi/\lambda$) and the plasmonic zone (near-field, $k > 2\pi/\lambda$), respectively. The plotted points indicate all scattering modes corresponding to phase change per a period of the staggered corrugation. These non-localized waves travel around and radiate in free space, and therefore have no interaction with the particle beam. The global band-gap noticeably emerges from $\omega a/2\pi c = 0.265$ to $\omega a/2\pi c = 0.31$ at either the photonic or plasmonic wave area. There is no other photon mode than interactive plasmon modes in the first forbidden band. The channel confined interaction modes disappear beyond the stop-band as they radiate to annihilate in free space owing to the non-resonant matching condition with the crystal lattices. Note that the PBG-modes are considerably more dispersive than fundamental eigenmodes of the conventional oversized grating waveguide (green-line). The fringe evanescent fields around the boundaries between the waveguide and the PBG-slabs distort the dispersion relation of the fundamental passband. These highly dispersive modes thus have larger group velocities with higher interaction impedances compared to the traveling-wave modes of the grating waveguide. Therefore, as the PBG-waveguide only supports propagation of the dispersive waves within the band-gap, the electron beam purely interacts with the active modes of $a/\lambda = 0.25 \sim 0.45$ and $\omega a/2\pi c = 0.265 \sim 0.31$ without exciting unstable wakefields.

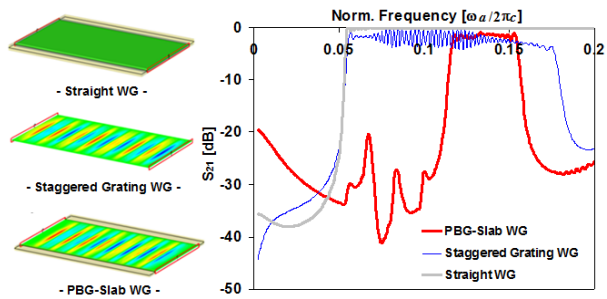

Figure 3: Transmission graphs through three types of accelerating waveguides.

Figure 3 exhibits transmission graphs (S_{21}) of three types of the slow wave structures: (a) straight waveguide, (b) grating-embedded channel, and (c) PBG-slab arrayed structure. Figure 3 shows that the fundamental passband of the asymmetrically corrugated waveguide, (b), ends at $\omega a/2\pi c \sim 0.35$, which corresponds to ~ 30 % instantaneous bandwidth, with ~ 2.5 dB insertion loss (~ 0.114 dB/mm attenuation at C-band). Modulation of the

ISBN 978-3-95450-115-1

wave traveling path degenerates photon energy states of confined EM waves due to their momentum divergence at the upper cutoff where localized fields longitudinally, rather than laterally, resonate with the periodic structure. On the other hand, transmission spectrum of the PBG-slab design clearly depicts that only the PBG-modes dominantly propagate through the traveling wave channel with nearly zero insertion loss, whereas all other modes beyond the band gap are completely suppressed below – 25 dB. Trapped wakefield modes irregularly arising from abnormal electron-photon coupling interactions could thus be intrinsically ruled out from the normal accelerating interaction.

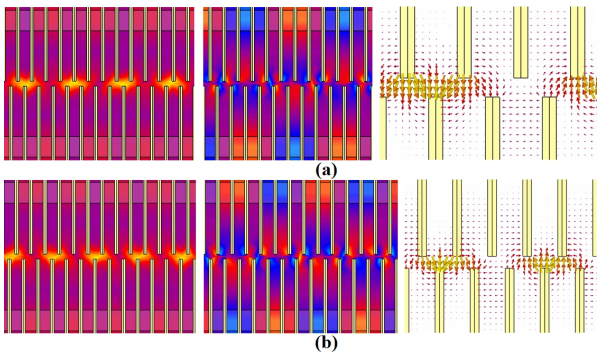

Figure 4: Transmission graphs through three types of accelerating waveguides.

Figure 4 displays 2D contour plots of electric field distributions (E_z) corresponding to the two interactive PBG modes, $a/\lambda = 0.25$ and $a/\lambda = 0.5$. While transverse fields (E_y) most dominantly appear in the channel, one can see that their field orientation is abruptly transitioned to the longitudinal direction between the two staggered vanes, accommodating sinusoidal field modulation of the axial field (E_z), which has constructive interaction with the electron beam with energy gain. It is noticeable that extended parallel conductor plates on account of the PBG slabs enhance capacitance of the resonance modes, leaking fringe fields of the longitudinal components. It may cause reduction of interaction impedances that could be compensated for by increasing the cross-sectional aspect ratio of the beam channel. The field gradient of the PBG-slab arrayed accelerating structure has been investigated with respect to frequency bands. Figure 5 shows axial field gradient graphs of the PBG-modes in terms of accelerating frequency bands, which are calculated with 50 kW driving power. For the scale analysis, all the geometrical dimensions of the designed accelerating structure are consistently reduced with the same ratio as the frequency increases. Note that the accelerating gradient is increased to ~ MV/m at W-band. Up-to-date modern klystron technology enables it to provide > 50 kW pulse power in the frequency range [13, 14], so that a high acceleration gradient of a few hundred MV/m would be achievable with the quasi-optical RF accelerating structure in THz regime.

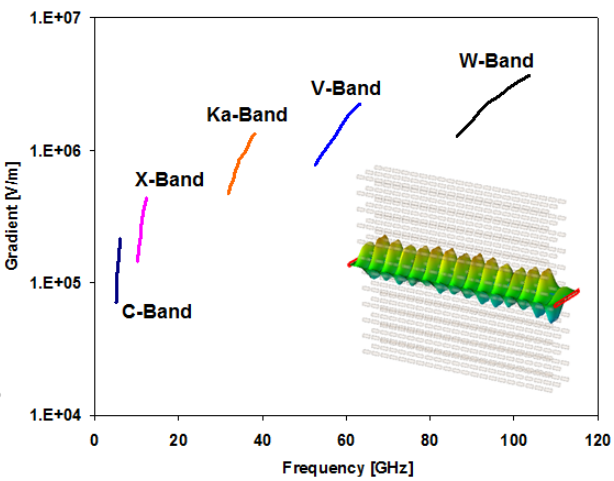

Figure 5: Acceleration gradients versus frequency bands of the PBG-slab structure (P_{in} = 50 kW).

CONCLUSION

In conclusion, EM simulations have revealed that the stagger-arrayed PBG-slabs enable to efficiently damp low-energy trapped modes and non-radiative HOMs in the planar RF accelerating structures and strongly support monochromatic propagation of PBG-modes. Embedding the photonic crystal structure selectively suppresses the fundamental passband below – 25 dB (C-band). The accelerating gradient gradually increases up to about a few MV/m level at W-band with 50 kW driving power and experimental investigation for further improvement is currently under consideration. The quasi-optically filtered RF structure supports stable mono-energetic bunching formation of an oversized flat beam, which can be utilized for high gradient accelerators and high power coherent radiation sources.

REFERENCES

[1] K. Mizuno and S. Ono, *J. Appl. Phys.*, vol. 46, no. 4, Apr. 1975
[2] X.-C. Zhang, Phys. Med. Biol. **47**, 3667 (2002)
[3] C. Sirtori, Nature Vol. 417, pp. 132 – 132, May 2002
[4] B. E. Carlsten, et. al. *Proceedings of the Seventh Workshop on High Energy Density and High Power RF* 807, 326
[5] M. E. Hill, R. S. Callin, X. E. Lin, and D. H. Whittum, SLAC-PUB-8666, Oct. 2000
[6] B. E. Carlsten, et. al., AIP Conf. Proc. 807, 326 (2006)
[7] L. Xiao, W. Gai, and X. Sun, Phys. Rev. E 65, 016505 (2001)
[8] Y.-M. Shin and L. R. Barnett, Appl. Phys. Lett. 92, 091501 (2008)
[9] Y.-M. Shin, L. R. Barnett, and N. C. Luhmann Jr., Appl. Phys. Lett. 93, 221504 (2008)
[10] E. I. Smirnova, et. al., J. App. Phys. **91**, 960 (2002)
[11] Evgenya I. Smirnova, et. al., Phys. Rev. Lett. 95, 074801 (2005)
[12] CST Microwave Studio version 2011
[13] Y.-M. Shin, et. al., IEEE Trans. Elec. Dev. 56, 3196 (2009)
[14] Y.-M. Shin, et. al., IEEE Trans. Elec. Dev. 58, 251 (2011)